Petroleum and Coal

Article **Open Access**

An Evaluation of Creep Strain under Varying Load Conditions in a Carbonate Formation

Uwaezuoke Nnaemeka, Obah Boniface

Department of Petroleum Engineering, Federal University of Technology, P.M.B 1526, Owerri, Nigeria

Received January 25, 2023; Accepted June 19, 2022

Abstract

Chalks are non-clastic type of carbonate sedimentary rocks. Any applied axial load would lead to a deformation of the sediments by the depletion of the pore fluids. This results in compaction which is a process in which the compressive strength of the rock is exceeded and plastic deformation occurs, resulting in irreversible reduction of porosity. In this work, a time-dependent deformation in chalks known as creep is presented. A reduction from 30 MPa to 5 MPa pore pressure in 100 minutes (0.25 MPa/min) was termed rapid loading. The same pressure was depleted for about 8333 minutes (0.003 MPa/min) and regarded as a slow loading. At the lower value of 5 MPa, the samples were left to deform under constant stress for some time. It was observed that when loaded rapidly, the deformation accumulated at the creep stage was higher; observed mainly at the transient creep phase, compared to when loaded slowly. The results of the experiments show that other parameters such as uniaxial compaction modulus both in the elastic and plastic regions, creep strain and creep rate are all loading-rate dependent. Hence, it could be inferred that if creep is porosity dependent, then it is load-rate dependent. Also, creep rate is highest for rapid loading and lowest for slow loading, while values for intermediate loading were in-between. The loading rate has to be widely different for variations in accumulated strains to differ with time.

Keywords: *Carbonate; Chalk; Creep rate; Creep strain; Uniaxial compaction.*

1. Introduction

In a producing oilfield, deformation is a result of interruption of loading. Similarly, compaction is a natural consequence of pore pressure depletion. However, it has been observed that there exists another kind of deformation that takes place when the state of stress in the rock skeleton is kept constant. This is known as creep, and it is a time-dependent deformation which may cause a delay in deformation response under varying load conditions. In other words, when production is interrupted in a field, strains continue to occur (creep), but this strain depends on the rate of production of the reservoir fluids. It has been established that when a reservoir is taken into production, the rate of change of the effective stress exerted on the reservoir rock is suddenly increased from that imposed by the burial process over a geologic time span, to that induced by the depletion pressure history [1].

Pure chalks are mainly built up of whole and fragmentary parts of calcite skeletons produced by planktonic algae [2]. The building blocks of the skeletons are calcite tablets or platelets of typical dimension 1 μ*m*. These calcite grains are arranged in rings or rosettes known as coccoliths, typically of the order of 10 μ*m* in diameter. Pure high porosity chalks consist of a mixture of intact coccoliths rings and greater and smaller fragments. This gives the chalk material a rather open structure, where the dimensions of the pore space may be considerably greater than the dimensions of the individual grains [3]. The mechanical properties of rocks (chalk) are functions of effective stresses as far as the following conditions are met;

- pore spaces are connected such that pore pressure is transmitted throughout the solid phase of the sample,
- pore fluid is inert in relation to the mineral constituents of the sample, and,
- permeability is enough for free flow of fluid in and out during deformation so that pore pressure gradient remains constant and uniform.

During withdrawal of fluids from hydrocarbon reservoirs, a considerable drop in the reservoir pore pressure occurs [4]. The weight of the overlying layers, known as the overburden, is carried partly by the reservoir fluid and partly by the rock skeleton [5-6]. This determines whether a rock would fail or not. It is known as the effective stress concept. As the pore pressure decreases, an increasing part of the constant weight of the overlying layers has to be carried by the reservoir skeleton. This resultant increased load leads to compaction until a new equilibrium is reached. This strain that acts vertically in the direction of the maximum principal stress is called the axial strain. However, a considerable compaction of the reservoir can be expected when one or more of the following conditions prevail [7]; production from large vertical interval significant reduction in reservoir pressure during the production period oil or gas, or both are contained in loose or weakly cemented rock.

Rock compaction can act as a very effective production mechanism (compaction drive) [8-10]. There exists depletion-induced compaction in sandstone reservoirs, and a model has been used to predict the compaction of sandstone reservoirs [1,11], but applying the model to chalk formations has proven to be more complex [1].

One method to determine the compaction potential is to utilize laboratory testing. By simulating conditions similar to field behavior, the response of the samples is measured. Obviously, laboratory conditions might differ from field conditions in several ways, for instance, the testing time might last for shorter time duration than the actual exposure time in the field. Also, testing equipment, assumptions and lack of knowledge of the field conditions are other possible sources of discrepancy between the field and the laboratory. But particularly, if lack of knowledge of the field is the issue, the conditions are based on assumptions or theoretical models. In most large hydrocarbon reservoirs, there is generally considered to be present a stress regime where compactional deformation occurs under conditions of no lateral strain, i.e. the reservoir will only experience vertical strain, usually referred to as uniaxial strain.

The objective was to investigate the effects of load rate on the creep behavior of a chalk formation (Stevns Klint), which study on it, has been done for compaction [12]. Both carbonates (chalk) and sandstones make up the major gas and oil reservoirs [13]. Core samples were loaded both rapidly and slowly and allowed to creep. The strains and creep rates are compared at the creep stage to check if the loading rate is the determining factor.

2. Materials and method

2.1. Materials

2.1.1. Laboratory apparatus

The apparatus used in the laboratory set-up and their functions are presented in Table 1.

Table 1. Laboratory apparatus and functions

Item		Function
1	Quizix QX pumps	Provides pressure on the confining chamber by pumping Bayol into the chamber already filled with same fluid
2	GILSON and ISCO pumps	To pump heptane as the pore fluid and build pressure to desired values
3	Linear Voltage Displacement Transducer (LVDT)	Measurement of piston's axial vertical movement, hence axial strain in the core samples
4	n-heptane	Pore fluid

Item		Function
5	Hydraulically operated triaxial cell	A chamber that houses the core sample (Figure 1), and makes application of pressures in three directions (triaxial) possible
6	Vacuum pump	To create vacuum in the pore spaces of the cores and also to saturate cores with pore fluid
7	Rosemount gauge	To display confining, pore and piston pressure readings
8	Lab-view program	To log data and monitor the test progress
9	Extensometer	To measure lateral expansion or contraction of the core diameter. It monitors the fluctuations in the radial deformation
10	Rubber rings	To prevent direct communication of the pore and confining fluids
11	Bayol	Confining fluid
12	Heat gun	To secure the core sample by welding the sleeve round the core

2.1.2. Equipment setup

The experiment was conducted in a rock mechanics laboratory using a hydraulically operated triaxial cell with the setup schematic shown (Figure 1). Figure 2 is a core sample properly positioned with an extensometer to monitor the lateral strain.

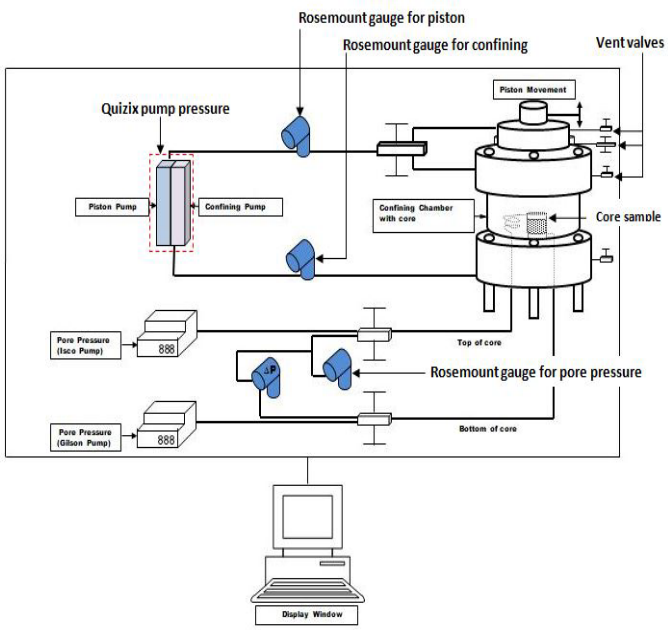

Figure 1. The laboratory setup (schematic)

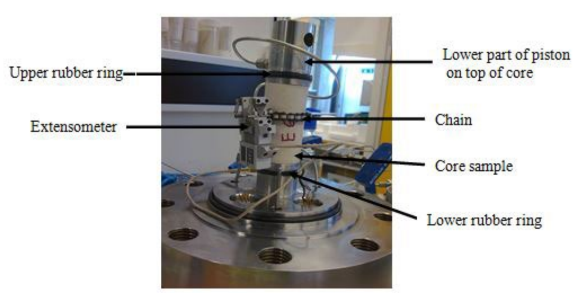

Figure 2. Positioning of core sample in the confining chamber of Figure 1

2.2. Method

Stevns Klint is a high porosity, pure outcrop chalk. Its porosity is usually above 40%. Twenty core samples were taken and cut into sizes. They were oven-dried for about 36 hours at a temperature of 130°C and weighed thereafter, giving the dry weight. Vacuum pump was used to suck out air and pore spaces later filled with the heptane and measured as wet weight. The information was used to determine the porosities of the core samples; since the volume of the fluid in the pore-filled spaces gives a direct indication of the pore volume for porosity determination.

Subsequently, core samples were taken to overburden, confining and pore pressures using the cores in the triaxial cell chamber as shown (Figure 1). The overburden was achieved by running down the piston against the core samples, while the confining and pore pressures were achieved using the Quizix and GILSON/ISCO pumps, respectively. The pore pressure was then depleted from the initial state to a certain value. This reduction results in an increase in the effective stresses, which then activates a certain behavior of the chalk grains. The behavior of the grains is affected by the rate at which the stress is increased. Hence, samples are loaded both rapidly and slowly and deformation and other parameters are thereafter compared. Intermediate loading rate between the rapid and slow loading rates is also included to investigate the behavior towards the two extremes.

The experiment involves tests in which the different loading rates are applied under the same stress conditions. Both confining and pore pressures were built up simultaneously from 1.2 MPa and 0.2 MPa, respectively, to the desired levels with a margin of 1MPa at confining pressure of 31MPa and pore pressure of 30MPa. The confining pressure represents the lateral stresses (x and y directions) in a reservoir, but since the test is uniaxial, the stresses in the lateral directions are considered equal due to cylindrical cores in an hydraulic confining chamber, with only axial deformation and no (negligible) lateral deformation. The overburden pressure of 32 MPa is provided by a piston running down from the top of the uniaxial compression test cell plus an additional effect of the confining fluid taken care of by relevant friction and area factors. In carbonates (chalk), creep is common and how the rate of loading affects creep and creep rate has been investigated. The tests for creep in this research were performed under drained conditions (constant pore pressure).

Moreso, the triaxial test was performed by taking the vertical and the horizontal stresses to a level (hydrostatically loading), and thereafter keeping the radial stresses at a constant value or level as the vertical or axial stress is increased, and measuring the compaction, ε_z, and the radial strain, ε_r, as the axial stress is increased. It requires fewer control variables than the uniaxial strain test, thus easier to carry out. It gives the ability to establish failure criterions, and the Young's modulus can be calculated at any desired period of interest. The uniaxial strain test performed is a standard test performed by keeping the radial displacement or deformation of the sample at a constant value ± 0.01, allowing only the sample to compact axially or vertically. This is commonly used in the laboratory, with the assumption that it is the most suitable method of simulating field behavior. It is not unusual to combine the uniaxial strain test with a creep test; hence this study was based on such a combination. The uniaxial strain test is applied in quantifying the immediate load response of the material. By correlating the creep response in the laboratory to a depletion rate of the pore pressure, the total compaction can be calculated.

3. Results and discussion

The results of the work are presented and discussed to highlight observations under specified assumptions. As shown in Table 2, the lengths and diameters of the core samples were measured and used together with the other parameters in Table 2 to calculate the porosities of the core samples used in the experiments [14].

Table 2. Initial porosity table/calculation

Core name	Length [mm]	Diameter [mm]	Weight, [g]			Bulk Volume [cm^3]	Pore Volume [cm^3]	Porosity [%]
			Dry	Wet	ΔWt.[g]			
E1	80.50	38.10	141.16	180.58	39.42	91.79	39.42	42.95
E2	79.65	38.15	139.36	178.44	39.08	91.06	39.08	42.92
E3	78.95	38.10	139.56	176.81	37.25	90.02	37.25	41.38
E4	80.00	38.10	140.01	179.45	39.44	91.22	39.44	43.24
E5	80.50	38.10	140.09	180.03	39.94	91.79	39.94	43.51
E6	79.15	38.15	145.49	182.07	36.58	90.49	36.58	40.43
E7	80.00	38.15	141.01	180.66	39.65	91.46	39.65	43.35
E8	78.30	38.10	137.25	175.5	38.25	89.28	38.25	42.84
E9	79.50	38.10	140.75	179.42	38.67	90.65	38.67	42.66
E10	79.00	38.15	139.49	178.19	38.70	90.32	38.70	42.85
E11	79.95	38.15	134.88	174.62	39.74	91.40	39.74	43.48
E12	80.00	38.20	141.19	180.8	39.61	91.70	39.61	43.20
E13	73.65	38.15	134.35	168.48	34.13	84.20	34.13	40.53
E14	79.95	38.10	138.27	177.29	39.02	91.16	39.02	42.80
E15	80.00	38.15	139.23	178.77	39.54	91.46	39.54	43.23
E16	79.65	38.15	141.77	179.26	37.49	91.06	37.49	41.17
E17	79.85	38.10	138.36	177.77	39.41	91.05	39.41	43.28
E18	79.65	38.10	138.3	177.7	39.40	90.82	39.40	43.38
E19	80.00	38.15	138.95	178.76	39.81	91.46	39.81	43.53
E20	76.90	38.10	132.59	170.67	38.08	87.68	38.08	43.43
Average	79.26	38.13						42.71

Table 3. Creep strains for rapid loading

Core name [rapid loading]	Creep strain [%]		
	500 min.	1000 min.	2000 min.
E2	1.00	1.23	1.55
E4	0.74	0.78	0.82
E13	0.15	0.16	0.17

Table 4. Creep strains for intermediate loading

Core name [intermediate loading]	Creep strain [%]		
	500 min.	1000 min.	2000 min.
E8	0.38	0.41	0.48
E11	0.31	0.36	0.40
E12	0.28	0.29	0.31
E16	0.28	0.30	0.31

Table 5. Creep strains for slow loading

Core name [slow loading]	Creep strain [%]		
	500 min.	1000 min.	2000 min.
E3	0.21	0.33	-
E14	0.068	0.085	0.096

Tables 3, 4 and 5 show the creep strains observed for core samples indicated at rapid, intermediate and slow loading rates.

3.1. Creep strains

There are clear differences between the strains observed at the creep phases under the different loading scenarios. There appears to be a connection between the strain at the loading phase and the strain at the creep phases. When higher strain is exhibited at the loading phase, there tends to be a lower strain at the creep phases and vice versa. From Figure 3 for rapid loading (core E2), the strain observed during the loading (when the effective stress was increased by depleting the pore pressure) was lower compared to that observed during the slow loading. But at the creep phase, as seen in Figure 4, there was a significant difference in the strains on both scenarios. The rapid loading showed a rapid strain especially in the transient (primary) creep phase, followed by a reduced strain at the region described as the steady state or (secondary) creep stage. At about 500 minutes of normalized creep time into the creep phases, the strain in the rapid loading is 1% as shown in Figure 5 for rapid loading. There was no accelerating (tertiary) creep stage observed in the creep strains.

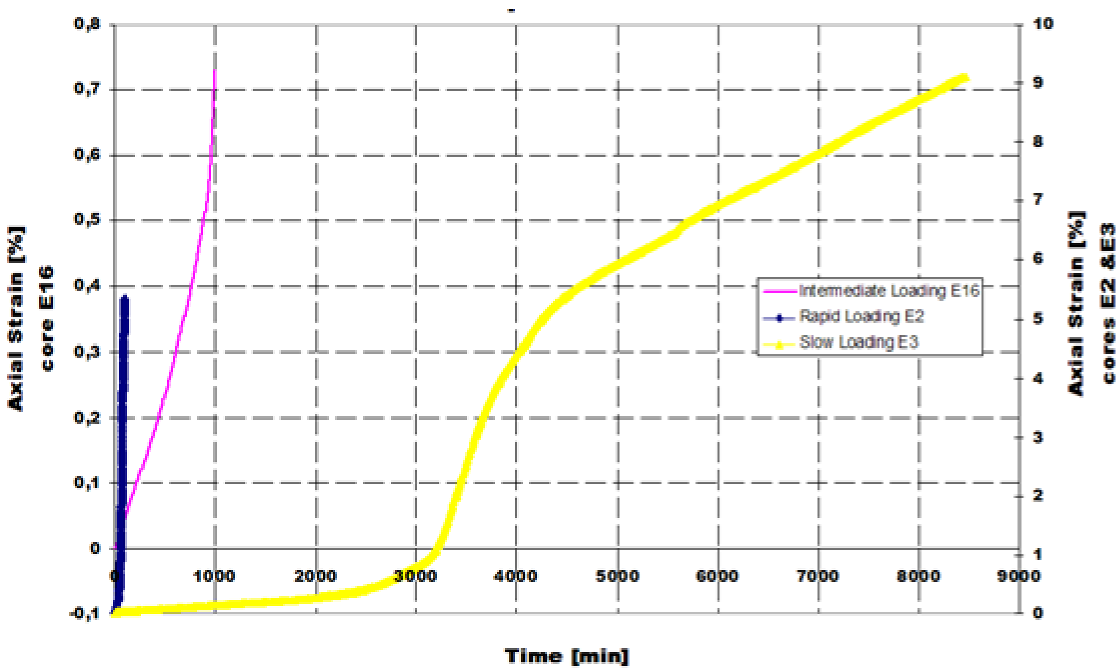

Figure 3. Comparison of the strains observed for slow [E3], rapid [E2] and intermediate [E16] loading scenarios during pore pressure depletion

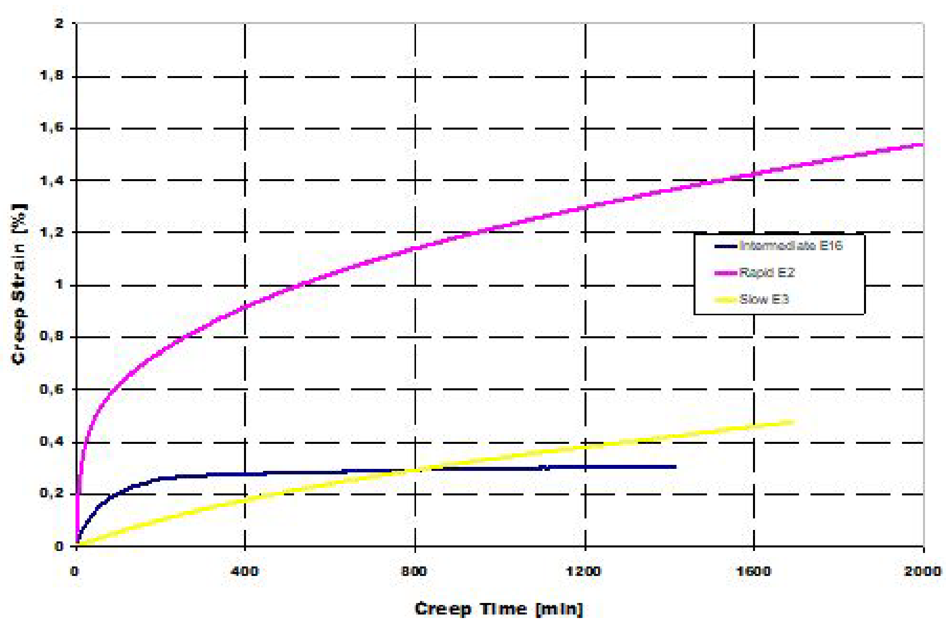

Figure 4. Comparison of the creep strains observed for slow, rapid and intermediate loading scenarios

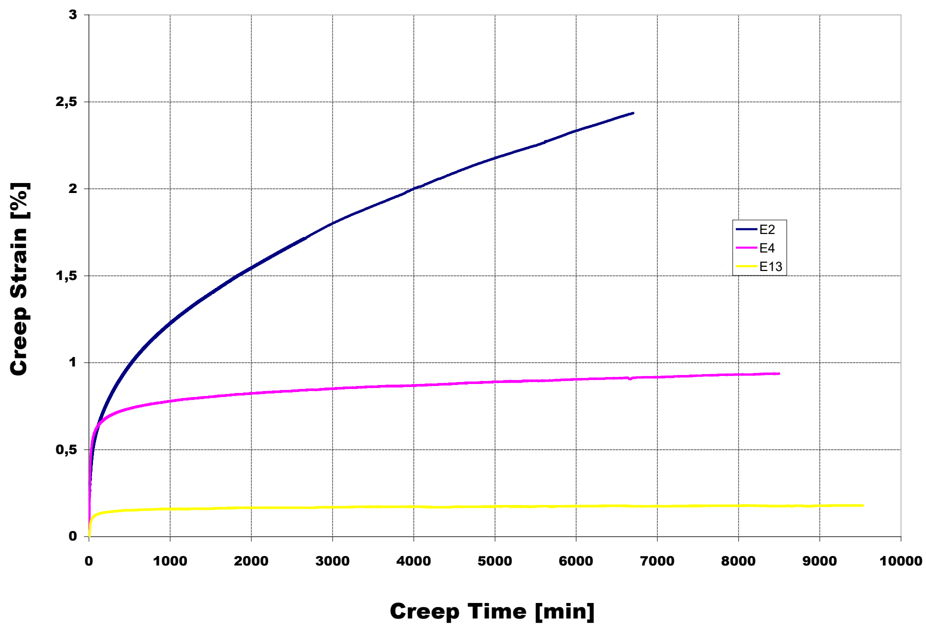

Figure 5. Creep strain for rapid loading of E2, E4 and E13

For slow loading (core E3) in Figure 6, there appeared to be a lower strain and also a less rapid change in strain in the transient creep stage compared to the rapid loading. At about 500 minutes of normalized creep time into the creep phases, the strain in the slow loading is 0.20%. If this is compared with the strain in the rapid loading test, one could see a factor of 1:5. Though the ratio reduces as we get into the next stage (secondary phase), it shows that the creep strain, under different loading conditions is significantly high to be given some due considerations. Within the same period, the strain observed in the core used for intermediate loading in this case (core E16) seems to have stabilized at a value of 0.3% when compared with the others, though a closer look by zooming into the plot shows that the material still creeps at a low rate. The creep strain observed in this case expectedly falls between the rapid and slow loading scenarios. The high creep was observed in the transient phase while the stabilization could be said to represent a state of low creep strain rate. It raises questions on the factors that contribute to this variation in the creep behavior of chalk under different loading rates. The porosities fall within the same range and hence might not be the differentiating factor. The effect of porosity could be investigated if the same load rate is used to test the cores so that variations could be accounted for by, maybe, also including the pore volumes.

As it is obvious that the cores had already yielded before the start of this creep period, it was considered to look at the behavior of the chalk after yield together with the behavior before yield (elastic) to account for this observation. Though compaction has been defined as the irreversible reduction of porosity after compressive strength has been exceeded, the additional deformation and reversible reduction in porosity before yield are taken into account [8]. This is done by calculating the strain from the start of depletion where loading of the cores are started (increase in effective stress). Since yield stress is higher for rapid loading than for slow loading, an onset of yield earlier in slow loading is accompanied by a sharp decrease in porosity and hence strains in the depletion phase that occur after yield begins earlier in slow loading. The material then deforms more in the longer time spent in the loading phase. This leads to a less strain observed during the creep phase. Whereas for the rapid loading, the higher yield stress and short time does not permit strain enough to be seen in the depletion phase rather this is observed in the creep phase mainly at the transient creep stage, due to the viscoelastic properties of the chalk grains. There appears to be a delayed response in the stress (pressure) changes during depletion. The delayed response is exhibited in the creep stage resulting in higher creep. Although this phenomenon happens also in the slow loading, the extra time allowed in this test for the loading allows for the viscoelastic behavior to be exhibited. Then more strain is observed during the loading phase, and in the creep phase, a lower value of strain then results. It is noteworthy to say that the strain is a combination of several factors.

Figure 6. Creep strain for slow loading of E3 and E14

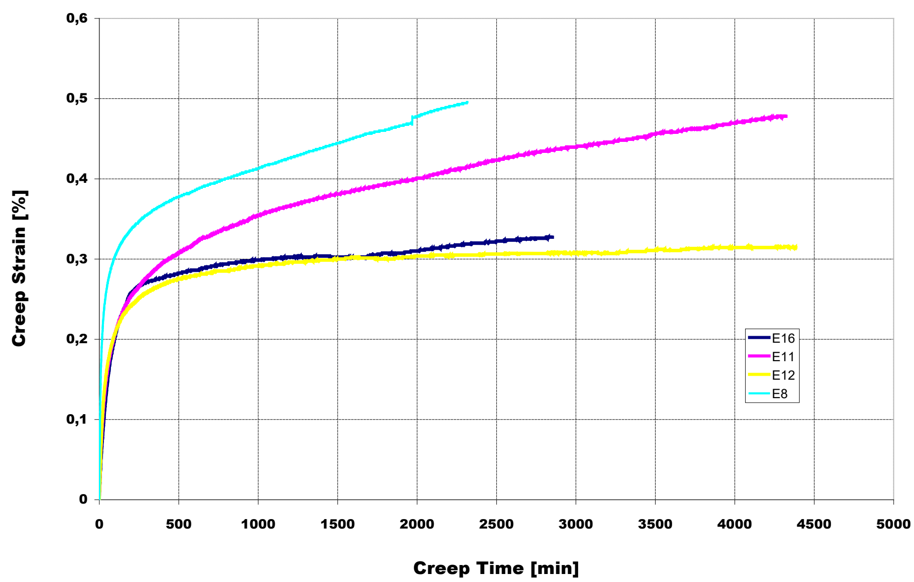

Figure 7. Creep strain for intermediate loading with cores E8, E11, E12 and E16

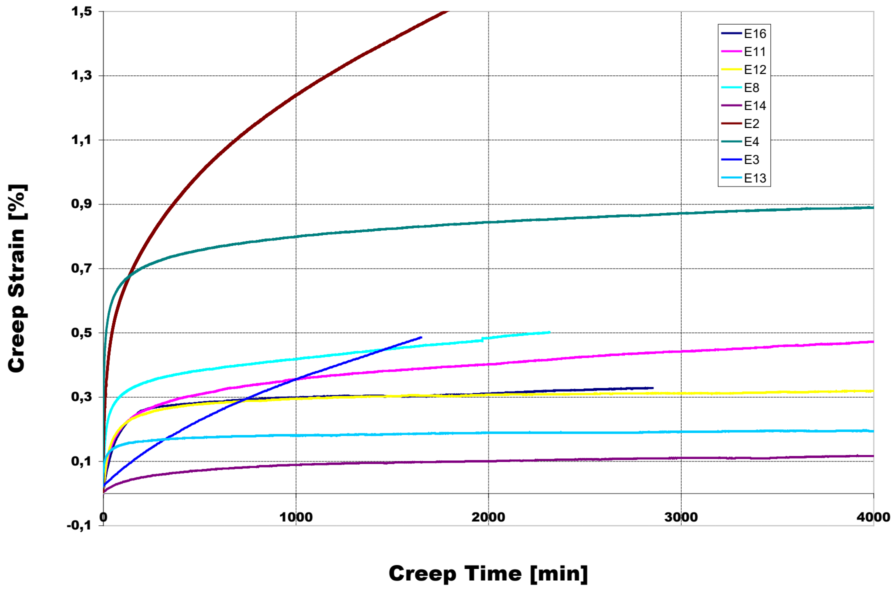

Figure 8. Creep strain for different loading rates used in the test; rapid loading [E2, E4 and E13], intermediate loading [E8, E11, E12 and E16] and slow loading [E3, E14]

Considering creep strain from another perspective, in that the yield of chalk causes a mobilization of the grains as the cementation is broken, and materials begins to re-orient in position. The dislodged particles then migrate through the porous, fluid-filled medium, though facing some resistance from the fluids, unto other locations until they come to a point of rest. This point of rest prohibits further movement unless the bounding particles are themselves shifted. That would often be the case as loading continues. Then, there tends to be an ever continuous migration of particles a far as there remains a porous (and permeable) medium. This particle movement happens through the matrix permeability and even enhanced by the presence of micro-cracks which are developed as strain continues. It is then deduced that creep is an 'everlasting phenomenon' especially in high porosity materials (chalk) which still retains high porosities, for instance 38.10 % at 5 MPa pore pressure after some creep period. From Figures 5 and 6, it is seen that the trend already established from the start of the creep signals continuous creep strains with time, though for slow loading, the curve is more linear (E3) from the beginning which shows less variation of strain at the various stages. This observation has been reported and several models exist that tend to predict how the curve would behave over a long period of time. Also shown in Figure 7 are creep strains for intermediate loading of core samples.

The Figure 8 shows the comparison of the creep strain of some cores which shows that for intermediate loading, the creep strains falls between rapid and slow loading cases. Though core E14 seems not to show any strains after about 1000 minutes of creep time from the plot, one might conclude that creep does not last for slow loading. Re-scaling of the plot would show the similar trend with the others. It is observed that creep behavior of chalk is load rate dependent and the degree of variation of different samples at a particular load rate. For example, rapid loading depends on the peculiar properties of the sample used. If the plot is separated into transient and steady-state phases of creep, it would be observed that the curves are more comparable in the transient than in the steady-state where it appears like some cores have stabilized and begins to creep alike in terms of trend. Models have been used to predict the persistence of the trends with time [15].

If we assume that cores E4 (rapid loading), E11 (intermediate loading) and E14 (slow loading) are comparable, then after about 500 minutes of normalized creep time which observably falls within the transient phase, the creep observed are 0.74125%, 0.31019% and 0.06875%, respectively. Hence, the core loaded rapidly had creeped in excess of 10 times than that loaded slowly and 2 times that of intermediate.

After 1000 minutes of normalized creep time, it had creeped about 9 times as much as that in slow loading and 2 times that in intermediate and after 2000 minutes, about 8 times as much as slow loading and 2 times that of intermediate. If the intermediate and slow loadings are compared at the different times as deduced, it is found that the intermediate has the same excess strain of 4.

3.2. Creep rates

This is the observed rate of creeping over a time interval. It is extracted from the creep strain versus time plot and could be presented as strain [%] per hour, minute and decade. One approach as shown in Figure 9 is by making a plot of the creep strain and the logarithm of time and obtaining the slope of the linear part (usually end) of the curve.

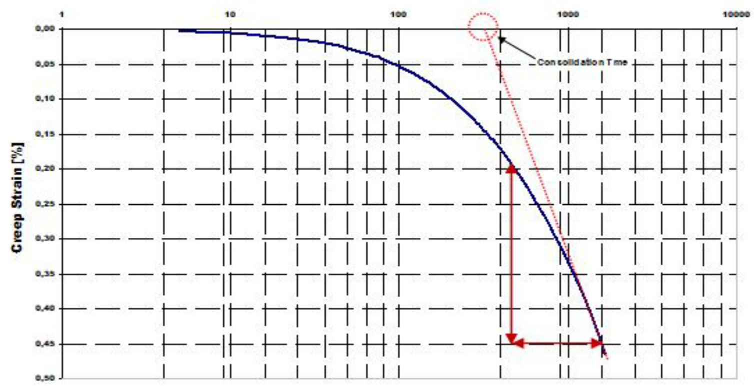

Figure 9. Determination of creep rate

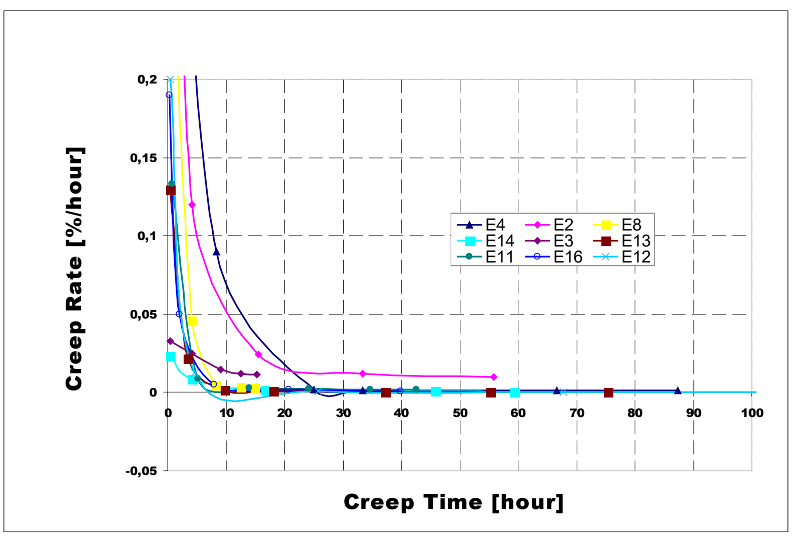

Figure 10. Plot of creep rate versus time

It then becomes evident that enough data needs to be logged to be able to have a good curve to produce the linear side of the curve. Inadequate data points produces a continuous curve that never converges due to consolidation, hence no linear part might be seen. A projection of this linear part of the curve unto the time axis yields the consolidation time, which is the time used for the pore pressure equilibrium to re-equilibrate. It is observed that this consolidation time decreases with the various creep periods introduced after each cyclic phase. These cycles serves to agitate and repack the chalk grains, though without re-establishment of the initial porosities.

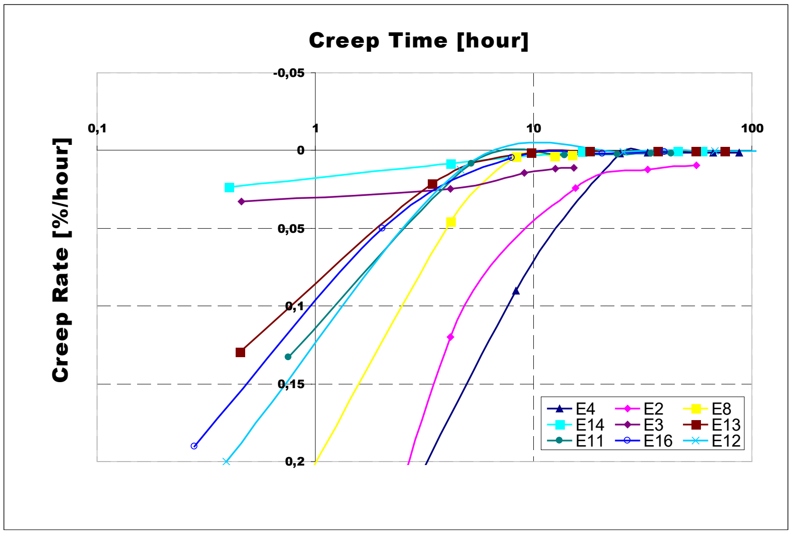

Figure 11. Plot of creep rate versus log of time for rapid loading [E2, E4 and E13], intermediate loading [E8, E11, E12 and E16], and slow loading [E3, E14

Another approach is to choose points from the normalized creep strain versus time curve and find the slopes and make plots as desired as shown if Figure 10. It is observed that core samples E2 and E4 used for rapid loading have the highest creep rates before stabilizing at nearly constant creep rate, though E13 behaved differently; while samples E3 and E14 used in slow loading have the lowest creep rates prior to stabilization. Samples E8, E11, E12 and E16 are used for intermediate loading, and all fall between those of rapid and slow loading. It is noteworthy that stabilization in this context means close to constant creep rate. Also, all the three curves for intermediate loading later intersected those of slow loading before stabilization and the rate curves for slow loading showed signs of stabilization earliest. Generally, creep rate decreases with time at a very high rate at the start of the creep and then stabilizes after a time. One might say that the creep rate becomes constant after some time. It then follows that a material creeps as far as there is porosity and none of the samples stopped creeping as long as the tests were kept running. From Figure 11, the creep rate is plotted against the log of time. It is observed that the rates tend to converge after some time irrespective of the load rate with the slow and intermediate loading converging earlier than that of rapid loading. One could then say that the intermediate load rate (0.025 MPa/min) used in the test results in behaviors of the sample that tend towards the behavior of slow loaded materials in terms of creep rate. If another intermediate rate closer to rapid loading is used, the result should confirm if the rate should clearly separate or tend towards rapid loading.

4. Conclusion

A change of load rate from lower to higher pressure gradient for different tests would result in an apparently higher stiffness. It was observed that application of loading cycles in the creep phases affected the compaction behavior. This loading cycle involved increasing (unloading) and decreasing (loading) the pore pressure, as the effective stress was decreased and increased, respectively. In the process, grains were agitated, re-oriented and re-packed. As a result, they became stiffer and strained less. It was observed that the introduction of the cycles did not reverse the porosity already lost during the depletion phases. Similarly, consolidation time changed with application of more load cycles, the result showing a downward trend or decrease in consolidation time with more load cycles. This was because the material became stiffer as stated previously after every cycle phase. It therefore took lesser time for the pore pressure equilibrium to re-equilibrate (consolidation). Moreso, there was more loss of porosity during pore pressure depletion in slow loading compared with rapid loading from the start of depletion to the end (beginning of creep). Hence, it could be inferred that if creep is porosity dependent, then it is load rate dependent. Also, creep rate is highest for rapid loading and lowest for slow loading, while that for intermediate loading are between. The loading rate has to be widely different for variations in accumulated strains to differ with time.

Assumptions

i. *Uniaxial compaction*
ii. *Elastic rock behavior*
iii. *Biot's factor of 1 for chalk*
iv. *No lateral deformation (constant core diameter)*

Acknowledgement

This work was carried out as part of Master of Science (M.Sc) research at the University of Stavanger, Norway's rock mechanics laboratory. The naming of the core samples is consistent with the thesis.

Declaration of competing interest: *No conflict of the interest has been declared by the authors*

References

[1] de Waal JA. On the rate type compaction behavior of sandstone reservoir rock, Thesis at The University of Delft, 1986. Retrieved from:http://resolver.tudelft.nl/uuid:b805782b-2eb4-4f72-98f4-f727c4ea9df0
[2] Risnes R, Flaageng O. Mechanical properties of chalk with emphasis on chalk-fluid interactions and micromechanical aspects. Oil & Gas Science and Technology – Revue de IFP, 1999; 54(6): 751-758. http://dx.doi.org/10.2516/ogst:1999063
[3] Risnes R. Deformation and yield in high porosity outcrop chalk. Physics and Chemistry of the Earth, Part A: Solid Earth and Geodesy, 2001; 26 (1-2): 53–57. https://doi.org/10.1016/S1464-1895(01)00022-9
[4] Aadnøy BS. An introduction to petroleum rock mechanics, rock mechanics compendium, Revised, 2003.
[5] Terzaghi, K. Theoretical Soil Mechanic. Wiley, New York, 1943: http://dx.doi.org/10.1002/9780470172766
[6] Fjær E, Holt RM, Horsrud P, Raaen AM, Risnes R. Petroleum related rock mechanics, 2nd Edition. In Developments in Petroleum Science 53, Elsevier 2008.
[7] Geertsma J. Land subsidence above compacting oil and gas *reservoirs.* J Pet Technol., 1973; 25: 734–744. https://doi.org/10.2118/3730-PA
[8] Settari A. Reservoir compaction. Journal of Petroleum Technology, 2002; 54 (8): 62–69. https://doi.org/10.2118/76805-JPT
[9] Geilikman MB, Wong SW. Oil and gas reservoirs compaction - induced production decline - influence of rock parameters. Paper presented at the 11th ISRM Congress, Lisbon, Portugal, 2007.
[10] Chan AWK. Production-induced reservoir compaction, permeability loss and land surface subsidence. Ph.D Dissertation, Stanford University, 2004.
[11] Hol S, Dudley JW, van der Linden A.J. New global correlations to assess depletion-induced compaction of progressively-buried sandstone. Paper presented at the 53rd U.S. Rock Mechanics/Geomechanics Symposium, New York City, New York, 2019.
[12] Fabricius IL. Compaction of microfossil and clay-rich chalk sediments, Physics and Chemistry of the Earth, Part A: Solid Earth and Geodesy, 2001; 26(1-2): 59-62: https://doi.org/10.1016/S1464-1895(01)00023-0
[13] Javid A, Hossein T. Investigating of petrophysical and lithological parameters of Asmari formation in Bibi-Hakimeh oil field, SW of Iran. Petroleum and Coal, 2019; 61(4): 855-859.
[14] Uwaezuoke N. Creep behavior and loading rate dependency of chalks. Master of Science Thesis, University of Stavanger, Norway, 2009. http://hdl.handle.net/11250/183420
[15] Omdal E, Madland MV, Kristiansen T, Nagel N, Korsnes R, Hiorth A. Deformation behavior of chalk studied close to in situ reservoir conditions. Rock Mechanics and Rock Engineering. 2010; 43(5): 557-580. https://doi.org/10.1007/s00603-010-0087-4

To whom correspondence should be addressed: Dr. Uwaezuoke Nnaemeka, Department of Petroleum Engineering, Federal University of Technology, P.M.B 1526, Owerri, Nigeria, E-mail: nnaemeka.uwaezuoke@futo.edu.ng ORCiD: https://orcid.org/0000-0002-4729-4072